Forward Experiments at LHC

Alessia Tricomi[1]

[1]University of Catania and INFN Catania, Catania, Italy

Observations of Cosmic Rays over a wide energy range provide useful information to understand high energy phenomena in the Universe. Large experiments for the detection of secondary particles produced in the interaction of primary Cosmic Rays are providing valuable inputs and progress in the field. However, the uncertainty caused from the poor knowledge of the interaction between very high energy primary cosmic ray and the Earth's atmosphere prevents the deduction of astrophysical parameters from the observational data. The Large Hadron Collider (LHC) provides the best opportunity for calibrating the hadron interaction models in the most interesting energy range, between 10^{15} and 10^{17} eV. To constrain the models used in the extensive air shower simulations the measurements of very forward particles are mandatory. Among the LHC experiments, measurements expected by TOTEM, ZDCs and LHCf will give crucial forward particle data for cosmic ray studies. In this paper, the impact of LHC forward experiments for Cosmic Ray Physics is discussed.

1 Introduction

The capability to measure the energy spectrum, the arrival direction and the chemical composition of the cosmic rays reaching Earth's atmosphere is of fundamental importance to understand the origin of High Energy Cosmic Rays and the high energy phenomena happening in our Universe. Despite in the last decades a huge step forward in the understanding of High and Ultra High Energy Cosmic Rays (UHECR) has been achieved thanks to large Extensive Air Shower experiments (EAS), still the origin and nature of cosmic rays with energies between 10^{15} eV and the Greisen-Zatsepin-Kuzmin (GZK) cutoff at about 10^{20} eV, remains a central open question in high-energy astrophysics. In fact, due to the low observed flux of high energy primary cosmic ray (Fig. 1, left), no direct measurement is possible and primary cosmic ray properties can be inferred only by indirect (yet complementary) measurements of shower particles produced in the interaction with the atmosphere which acts as a "calorimeter" medium. The first method relies on measuring the fluorescence light emitted by air molecules excited by the cascade of secondaries. The second one relies on the use of either water Čerenkov tanks or scintillators to sample the shower at ground. However, the interpretation of EAS data in terms of primary cosmic ray properties is not straightforward since it is strongly affected by the knowledge of the nuclear interactions in the Earth's atmosphere and results are not always in agreement between different experiments. This is true, for instance, for the determination of the primary energy spectrum in the UHE region, in particular the existence of events above the so called GZK cut-off, and the chemical composition of cosmic rays. Contradictory results have been reported for the existence of events over the GZK cut-off. Indeed, evidence of such UHECRs, above the cut-off, have been reported by the AGASA experiment [1], while the results of the HiRes [2] experiment and, more recently, the ones of the Pierre Auger Collaboration [3] are consistent

with the existence of the cut-off. A key point which raises observing the cosmic ray energy spectra (Fig. 1) is the importance of the energy scale calibration between different experiments. As can be seen from Fig. 1, a systematic difference from the previous measurements is present also for the Auger results. It has been noted that with an energy rescale of AGASA, HiRes and Auger results most of the discrepancies disappear [4, 5, 6].

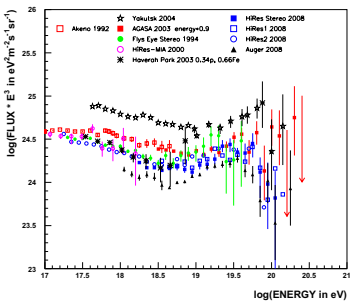

Figure 1: Energy spectrum of cosmic rays at the highest energies. A comparison of the results from main EAS experiments is shown. A clear discrepacy between AGASA, HiRes and Auger can be seen in the region above 10^{20} eV. From Ref. [5].

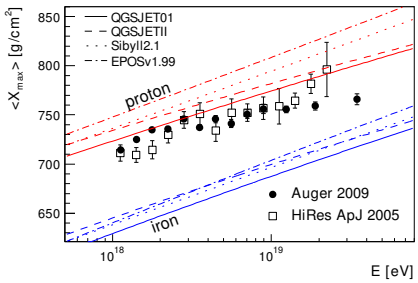

Figure 2: The position of the shower maximum X_{MAX} is shown as a function of the primary cosmic ray energy. The various lines correspond to predictions made by different Monte Carlo models. Plot from Ref. [7].

Similar considerations hold for the interpretation of cosmic ray chemical composition. Cosmic rays are not purely protons but they contain also heavy nuclei. Nuclear cascade showers initiated by the disintegration of heavy nuclei develop more rapidly in comparison with the showers initiated by protons. The position of the shower maximum, X_{MAX}, cleary depends on the composition of the cosmic rays.

Recently, Auger results pose another puzzle for the highest energy extra-galactic cosmic rays. Auger results on the correlation between the arrival direction of the cosmic rays and the direction of AGNs seem to indicate that the highest energy cosmic rays are protons [8] even if a subsequent analysis seems to indicate less correlation than what was claimed in the first paper [9]. On the other hand, florescence based measurements of air shower elongation seem to indicate that the composition of the highest energy cosmic-rays favour a mixed composition [10]. Fig. 2 shows a comparison of the most recent results on the X_{MAX} distribution as obtained by HiRes and Pierre Auger collaborations. Superimposed are the distribution expected by different Monte Carlo models [7].

Because the deduction of primary cosmic ray composition from the elongation parameter has a strong model dependence, especially in the highest energy region, the reduction of the uncertainty in the hadronic interaction models is important for solving this puzzle as for the correct interpretation of the primary spectrum. Accelerator experiments validating the interaction model chosen are hence mandatory. As a matter of fact air shower development is dominated by the forward products of the interaction between the primary particle and the atmosphere. The bulk of the primary particle production is dominated by forward and soft QCD interactions, usually modeled in Regge-Gribov-based [11] approaches with parameters constrained by the existing collider data ($E_{lab} \preceq 10^{15}$ eV). The only available data on the pro-

duction cross-section of neutral pions emitted in the very forward region have been obtained more than twenty years ago by the UA7 Collaboration [12] at CERN. They measured the photon distribution within an emission angle of as little as 1.8 milli-radians from the beam axis and up to an energy of 630 GeV in the center of mass system, corresponding to a laboratory frame energy of 2×10^{14} eV, well below the knee region. When extrapolated to energies around the GZK-cutoff, the current MCs predict energy and multiplicity flows differing by factors as large as three, with significant inconsistencies especially in the forward region. The LHC accelerator, thanks to its unprecedented energy of 14 TeV in the center of mass system, corresponding to 10^{17} eV in the laboratory reference frame, offers a unique opportunity to measure both neutral and charged particles emitted in the very forward region. It should be stressed that with LHC not only the energy frontier will be boosted but also, thanks to the complementarity of the different detectors installed, the capability to cover almost the full range of pseudorapidity will be reached (Fig. 3). Measurement of forward particle production in p-p, p-Pb, and Pb-Pb collisions at LHC energies will thus provide strong constraints on nuclear interaction models and allow for a better understanding of high energy cosmic ray properties.

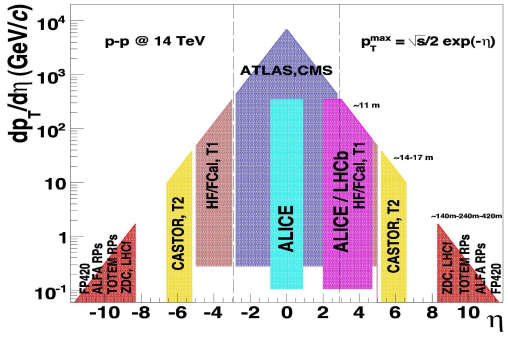

Figure 3: Acceptance in the $p_T - \eta$ plane of the current (and proposed) LHC experiments.

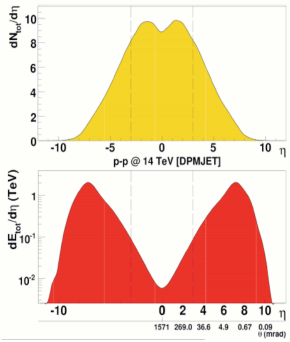

Figure 4: Total multiplicity (top) and energy flow (bottom) in 14 TeV p-p collisions at LHC.

2 Forward Physics at LHC

At LHC center of mass energy, secondary particles emitted in the forward direction (which are the bulk of the air showers) carry most of the energy (Fig. 4). Three fundamental parameters for air shower studies can be measured by accelerator experiments:

- Total/inelastic cross sections;
- elasticity/inelasticity;
- particle energy spectra.

The determination of these three parameters are mandatory to determine the longitudinal and lateral spread of air showers. Measurements near zero degree collision angle are also needed to determine the total cross section based on the optical theorem. In order to extend

the Physics program of general purpose detectors at LHC additional dedicated detectors for measuring the very forward particles produced in the collisions have been designed, as part of the major experiments or as independent experiments. The techniques used for measurement of the forward emitted particles can be classified into three different categories:

- detectors that surround the beam pipe in the forward region. In this case very forward particles remaining in the beam pipe cannot be covered;

- detectors inside the beam pipe that can be moved close to the beam. This is generally called the Roman Pot method after the Italian experiment that first employed this technique. This is the ideal method for measuring charged particles close to zero degree collision angle and is the standard method used to determine the total cross section via the optical theorem;

- detectors beyond the dipole separating the colliding beams and at zero degree collision angle (Zero Degree Calorimeters or ZDCs). This is the ideal method for measuring forward neutral particles since charged particles are swept out by the beam separation dipole and zero degree collision angle is accessible.

LHC experiments feature an unprecedented rapidity coverage thanks to dedicated forward detectors which complement the mid-rapidity coverage (Fig. 3). Both ATLAS [13] and CMS [14] has been instrumented also in the forward part. Forward calorimetry is available at ± 11 m (the FCal and HF hadronic calorimeters), at ± 14 m (CMS CASTOR sampling calorimeter) [15], and at ± 140 m (the Zero-Degree-Calorimeters, ZDCs) [16, 17] from Interaction Points (IPs). In addition, ATLAS has Roman Pots (RPs) at $\pm$ 220 and 240 m, and both ATLAS and CMS are planning to install a new proton-tagger system at 420 m (FP420) from each IPs. Also ALICE [18] and LHCb [19] are equipped with forward detectors: both have muon spectrometers covering the region $2 \preceq |\eta| \preceq 5$, not covered by ATLAS or CMS thus complementing their information. In addition, two independent forward experiments TOTEM [20] and LHCf [21] have been installed at LHC. TOTEM shares IP5 with CMS and it consists of two types of trackers (T1 and T2 telescopes) which surround the beam pipe covering the region $3.1 < |\eta| < 4.7$ and $5.2 < |\eta| < 6.5$ respectively, plus Roman Pots installed at ± 147 and ± 220 m covering the very forward ($\eta \sim 10$) elastically scattered particles that are near the outgoing beams. Combining these measurements, TOTEM can determine the total cross section with a precision of ± 1 mb. Last but not least, the LHCf experiment is a fully dedicated astroparticle experiment at LHC installed in the same region of the ATLAS ZDCs, ± 140 m away from IP1. The detector consists of two sampling and imaging calorimeters made by 16 layers of plastic scintillators interleaved by tungsten layers as converter. Additionally, a set of four X-Y position sensitive layers, made by 1 mm^2 scintillating fibers in one calorimeter and silicon micro-strip layers in the other, provide incident shower positions, in order to obtain the transverse momentum of the incident primary and to correct for the effect of leakage from the edges of the calorimeters. LHCf is a kind of ZDC, but designed with a very different concept from the ATLAS, CMS, and ALICE ZDCs. Like the ZDCs LHCf also measures the neutral particles emitted at and near zero degree collision angle. The single particle energy and position resolutions of LHCf have been optimized for discriminating between the hadron interaction models used in cosmic-ray studies.

3 Monte Carlo Model Discrimination

While the knowledge of nuclear interaction models is mandatory to infer primary cosmic ray properties from EAS experiments, unfortunately the bulk of particle production in high-energy hadronic collisions can still not be calculated from first-principles QCD. Monte Carlo models frequently used to simulate cosmic ray cascades, like DPMJET [22], QGSJET 01 and II [23], SYBILL [24] and EPOS [25], can be regarded as phenomenological "QCD-inspired" models. They are indeed based on general principles such as unitarity and analyticity often combined with perturbative QCD predictions for high-p_T processes to obtain an almost complete description of the final states. Soft processes are described within Gribovs Reggeon theory [11] and hadrons are produced mainly in the fragmentation of color strings. A detailed description of the difference between these models can be found in Ref. [26].

LHC data will play a fundamental role to calibrate all these models up to an energy of 10^{17} eV thanks to the complementarity of the forward detectors described in previous Section. In particular, data collected by TOTEM/ALFA and by LHCf/ZDC will be mandatory to achieve this goal.

The energy spectra of single γ-rays and neutrons expected to be measured by the LHCf experiment and calculated using the different hadron interaction models are shown in Fig. 5. In this calculation, a 1000 sec of the 14 TeV LHCf operation at a luminosity of $10^{29}\,\mathrm{cm}^{-2}\mathrm{s}^{-1}$ is assumed which will be achieved at the beginning of the LHC commissioning phase. 5% and 30% energy resolution respectively for γ and neutron and statistical errors are included in the calculation. As can be noted from Fig. 5 clear discrimination between the calculated spectra for the various models is possibile, especially for neutron spectra even if the energy resolution is significantly worse than for γ reconstruction. The measurement of forward neutron energy spectrum by LHCf/ZDC is of particular importance since it is related to the elasticity parameter discussed in Sect. 2 and can provide useful information to characterize the event in heavy ion collisions.

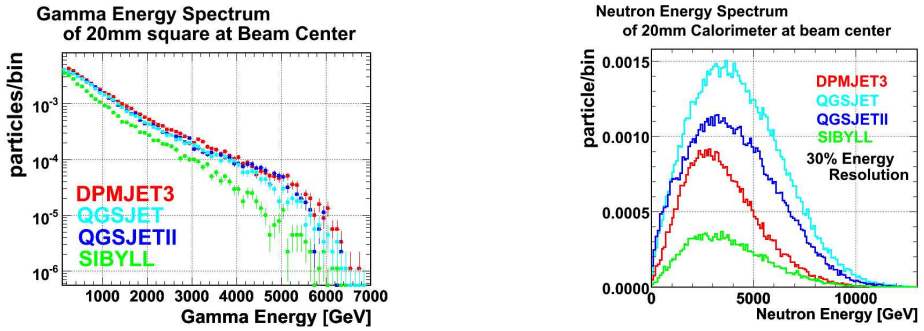

Figure 5: Expected energy spectrum for γs and neutrons according to different interaction models at 7+7 TeV center of mass energy. For γ a 5% energy resolution has been taken into account while for neutrons a 30% energy resolution has been included in the calculated spectrum.

The calibration of Monte Carlo codes asks for a precision measurement of the energy scale. For this reason LHCf relies on a very precise reconstruction of the π^0 mass, by reconstructing the 2 γ from π^0 decays each impinging one of the two towers of the calorimeter.

MC simulations for 1.04×10^7 and 1.17×10^7 p-p collisions, each corresponding to about 20 minutes operation during the LHC beam commissioning with 43 bunches and $10^{29}\,\mathrm{cm}^{-2}\mathrm{s}^{-1}$ of luminosity, were carried out with the DPMJET3.03 model for two different detector position (one in which the detector is in the nominal position and one in which the detector is 10 mm down), respectively. Details of the analysis can be found in [27]). As can be seen in Fig. 6, the reconstructed π^0 energy spectrum well reproduced the original production spectrum. A good discrimination between different Monte Carlo models is hence feasible.

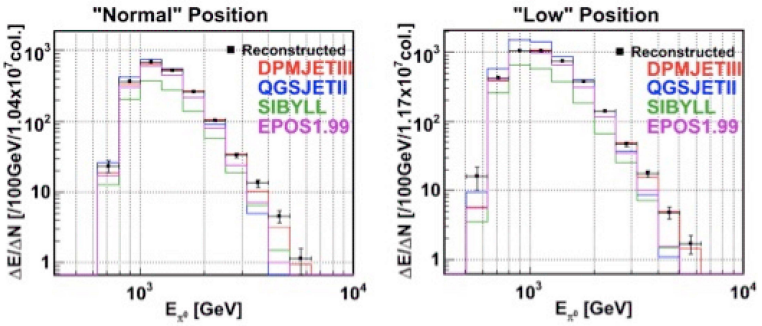

Figure 6: Reconstructed π^0 energy spectrum compared with expectations from different MC models for two LHCf detector positions. Events correspond to about 20 minutes at $10^{29}\,\mathrm{cm}^{-2}\mathrm{s}^{-1}$ luminosity for 14 TeV p-p collisions. The reconstructed spectrum well reproduce the production spectrum. The main systematic error is due to the uncertainty on the absolute energy scale of the calorimeter.

In addition to detecting $\pi^0 \to \gamma\gamma$ and forward going neutrons, the LHCf/ZDC can detect and reconstruct $\eta \to \gamma\gamma$ (Fig. 7 left), $\Lambda, \Delta \to n\pi^0$, $\Sigma \to \Lambda\gamma$ and $K^0_S \to \pi^0\pi^0$ (Fig. 7 right), and measure their production cross section, energy spectrum, and angle within the detector acceptance thus ensuring redundant tools for energy scale calibration.

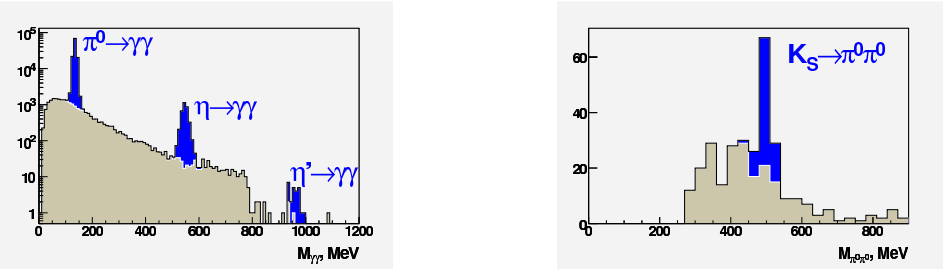

Figure 7: Simulated $\gamma\gamma$ (left) and $\pi^0\pi^0$ (right) mass spectra. Reconstructed π^0, η and η' peaks are clearly visible (left) above $\gamma\gamma$ background as well as K^0_S peak (right) above $\pi^0\pi^0$ background. Events corresponds to 10^6 p-p collisions at 14 TeV generated with Pythia 6.3. Plots from Ref. [16].

Figures 8 and 9 from Ref. [28] show for p-p collisions at 14 TeV and p+Pb collisions at 8.8 TeV, respectively, the inclusive multiplicity and energy flows predicted by the models for all

pseudo-rapidities, as well as the energy deposit in the acceptances covered by the CASTOR/T2 ($5.2 < |\eta| < 6.6$) and ZDC/LHCf ($|\eta| > 8.1$ for neutrals) detectors. In some cases, differences as large as 60% are observed between prediction of different models.

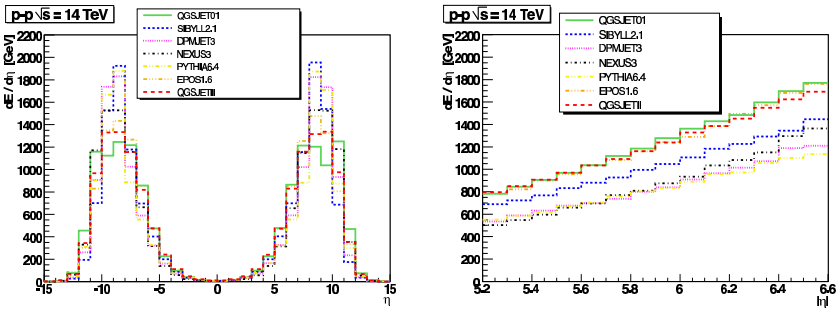

Figure 8: Energy flow in the whole pseudorapidity range (left) and in the CASTOR/T2 acceptance ($5.2 < |\eta| < 6.6$) (right) as predicted by different Monte Carlo models used in cosmic ray Physics for p-p collision at 14 TeV.

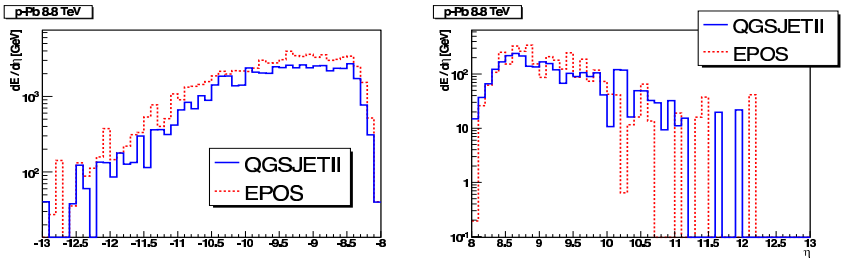

Figure 9: Neutral energy density in LHCf/ZDC acceptance for p+Pb collisions at 8.8 TeV as predicted by different Monte Carlo models used in cosmic ray Physics.

4 Conclusions

The new generation of HECR experiments provide valuable data to understand high-energy phenomena and, at the same time, pose interesting questions. To solve many of these puzzles the reduction of the uncertainty due to the hadron interaction model used in simulation is mandatory. Data collected at LHC will provide a fundamental instrument to calibrate Monte Carlo codes in the most critical energy range of the CR spectrum, between the knee and the GZK cut-off. In particular, LHC experiments feature an unprecedented rapidity coverage thanks to dedicated forward detectors which will provide the most significant data to discriminate the currently used models or set constraints for the future models.

Acknowledgements

I wish to thank all the people who helped me to collect useful material for this paper, especially O. Adriani, K. Eggert, D. D'Enterria, P. Grafström, M. Grothe and S. White.

References

[1] M. Takeda et al. Extension of the cosmic-ray energy spectrum beyond the predicted Greisen-Zatsepin-Kuzmin cutoff. *Phys. Rev. Lett.*, 81:1163–1166, 1998, astro-ph/9807193.

[2] R. Abbasi et al. Observation of the GZK cutoff by the HiRes experiment. *Phys. Rev. Lett.*, 100:101101, 2008, astro-ph/0703099.

[3] J. Abraham et al. Observation of the suppression of the flux of cosmic rays above 4×10^{19}eV. *Phys. Rev. Lett.*, 101:061101, 2008, astro-ph/0806.4302.

[4] V. Berezinsky. Transition from galactic to extragalactic cosmic rays. 2007, astro-ph/0710.2750.

[5] M. Nagano. Search for the end of the energy spectrum of primary cosmic rays. *New J. Phys.*, 11:065012, 2009.

[6] J. Bluemer, R. Engel, and J. R. Hoerandel. Cosmic Rays from the Knee to the Highest Energies. *Prog. Part. Nucl. Phys.*, 63:293–338, 2009, astro-ph.HE/0904.0725.

[7] M. Unger. Study of the Cosmic Ray Composition with the Pierre Auger Observatory. *Talk at SOCoR, Trondheim 2009*, 2009.

[8] J. Abraham et al. Correlation of the highest energy cosmic rays with nearby extragalactic objects. *Science*, 318:938–943, 2007, astro-ph/0711.2256.

[9] J. Abraham et al. Correlation of the highest-energy cosmic rays with the positions of nearby active galactic nuclei. *Astropart. Phys.*, 29:188–204, 2008, astro-ph/0712.2843.

[10] J. Abraham et al. Studies of Cosmic Ray Composition and Air Shower Structure with the Pierre Auger Observatory. 2009, astro-ph/0906.2319.

[11] V. N. Gribov. A REGGEON DIAGRAM TECHNIQUE. *Sov. Phys. JETP*, 26:414–422, 1968.

[12] E. Pare et al. Inclusive Production of $\pi^0 s$ and Feynman Scalin Test in the Fragmentation Region at the S $\bar{p}p$ S Collider. *Phys. Lett.*, B242:531–535, 1990.

[13] G. Aad et al. The ATLAS Experiment at the CERN Large Hadron Collider. *JINST*, 3:S08003, 2008.

[14] R. Adolphi et al. The CMS experiment at the CERN LHC. *JINST*, 0803:S08004, 2008.

[15] S. Basegmez et al. Performance studies of the full length prototype for the CASTOR forward calorimeter of the CMS experiment. CERN-CMS-CR-2008-090.

[16] Zero degree calorimeters for ATLAS. CERN-LHCC-2007-01.

[17] O. A. Grachov et al. Performance of the combined zero degree calorimeter for CMS. *J. Phys. Conf. Ser.*, 160:012059, 2009, nucl-ex/0807.0785.

[18] ALICE technical design report on forward detectors: FMD, T0 and V0. CERN-LHCC-2004-025.

[19] A. Augusto Alves et al. The LHCb Detector at the LHC. *JINST*, 3:S08005, 2008.

[20] G. Anelli et al. The TOTEM experiment at the CERN Large Hadron Collider. *JINST*, 3:S08007, 2008.

[21] O. Adriani et al. The LHCf detector at the CERN Large Hadron Collider. *JINST*, 3:S08006, 2008.

[22] Stefan Roesler, Ralph Engel, and Johannes Ranft. The Monte Carlo event generator DPMJET-III. 2000, hep-ph/0012252.

[23] Sergey Ostapchenko. Status of QGSJET. *AIP Conf. Proc.*, 928:118–125, 2007, hep-ph/0706.3784.

[24] R. S. Fletcher, T. K. Gaisser, Paolo Lipari, and Todor Stanev. SIBYLL: An Event generator for simulation of high-energy cosmic ray cascades. *Phys. Rev.*, D50:5710–5731, 1994.

[25] Klaus Werner. The hadronic interaction model EPOS. *Nucl. Phys. Proc. Suppl.*, 175-176:81–87, 2008.

[26] Klaus Werner. *These Proceedings*, 2009.

[27] Hiroaki Menjo. Simulation Study for the performance of the LHCf experiment. *Proc. of 31st International Cosmic Ray Conference, Łódź, Poland.*

[28] David d'Enterria, Ralph Engel, Thomas McCauley, and Tanguy Pierog. Cosmic-ray Monte Carlo predictions for forward particle production in p-p, p-Pb, and Pb-Pb collisions at the LHC. 2008, astro-ph/0806.0944.